High-transmittivity non-periodic sub-wavelength high-contrast grating with large-angle beam-steering ability

Changlian Ma (马长链)*, Yongqing Huang (黄永清), Xiaofeng Duan (段晓峰), and Xiaomin Ren (任晓敏)**

State Key Laboratory of Information Photonics and Optical Communications, Beijing University of Posts and Telecommunications, Beijing 100876, China

**Corresponding author: malian080250118@163.com;*

***corresponding author: yqhuang@bupt edu.cn*

Received July 23, 2014; accepted October 24, 2014; posted online November 28, 2014

We present a high-transmittivity non-periodic sub-wavelength high-contrast grating (HCG) with large-angle beam-steering ability for transmitted light. The phase front profile of transmitted light is a decisive factor to the beam-steering property of the HCG. By designing the structural parameters of the HCG, both beam steering and high transmittivity can be achieved. The properties of the beam steering and transmission are numerically studied with the finite element method. The results show that the transmittivity is up to 0.91 and the steering angle is 27.42° which is consistent with the theoretical 30°.

OCIS codes: 050.2770, 050.6624, 050.5080, 060.5060.
doi:10.3788/COL201412.120501.

High-contrast grating (HCG), which is 1D planar sub-wavelength structure with a high-refractive-index contrast[1–6], has been significantly developed in recent years. Because of the high transmittivity over a broad bandwidth and the property of controlling the phase shift of the transmitted light, HCG has emerged recently as a promising alternative to the conventional lens[7–10], especially in the field of integrated optics, such as vertical-cavity surface-emitting lasers (VCSELs)[11–14]. The integration of HCG will avoid using an external lens for collecting beam[15] (Fig. 1). If we want to get the beam emitted from the ordinary VCSELs chip arrays coupled into a collecting fiber, a lens is needed (Fig. 1(a)). But if the VCSELs chip has an ability of arbitrary-angle beam steering, there is no need to use an additional optical coupling lens (Fig. 1(b)). It is noted that every chip in Fig. 1(b) has the structure of HCG. The chip with small-angle beam-steering ability has been studied[15], but the transmission property is not satisfactory. So, it is necessary to study the chip with large-angle beam-steering ability and high transmittivity.

In this letter, we present a high-transmittivity HCG with large-angle beam-steering ability. The relationship between phase Φ of transmitted light at the transmission plane (Fig. 2) and x is derived in the first place. Based on this, we show how a non-periodic HCG pattern controls the phase front of the transmitted light beam, without affecting the high transmittivity. Properties of the proposed HCG are numerically studied with the finite element method (FEM)[16]. Simulation results show that the transmittivity is up to 0.91 and the steering angle is 27.42° which is in good agreement with the theoretically designed 30°.

Figure 2 shows a schematic diagram of beam steering. The electric field of the transmitted light can be written as

$$E(x,z) = E_0(x,z)\exp(\mathrm{j}k_0(x\sin\theta + z\cos\theta)), \tag{1}$$

where $E_0(x, z)$ is a power envelope, $k_0 = 2\pi/\lambda$ is the wavenumber at the wavelength λ, and θ is the angle between the wave vector of transmitted light and the negative z-axis. At the transmission plane, the z-axis coordinate is a constant, so the phase of the transmitted light at the transmission plane can be written as

$$\Phi(x) = k_0 x\sin\theta + c, \tag{2}$$

where c is a constant.

Equation (2) indicates that beam steering can be obtained if the phase response of the transmitted light at the transmission plane is linearly varying. Taking $\mathrm{d}\Phi/\mathrm{d}x$, we get

$$\Phi(x)' = k_0\sin\theta. \tag{3}$$

Figure 3 shows the schematic of the investigated HCG. The blue rectangles represent the high-refractive-index grating bars made of silicon, which are surrounded by low-refractive-index medium – air in our case. If the width of the non-periodic HCG is d, achieving a phase difference of $\Delta\Phi$, according to Eq. (3), we get a relationship as

$$k_0\sin\theta = \frac{\Delta\Phi}{d}. \tag{4}$$

By changing the form of Eq. (4), the steering angle θ can be obtained[15]

$$\theta = \arcsin\left(\frac{\Delta\Phi}{dk_0}\right). \tag{5}$$

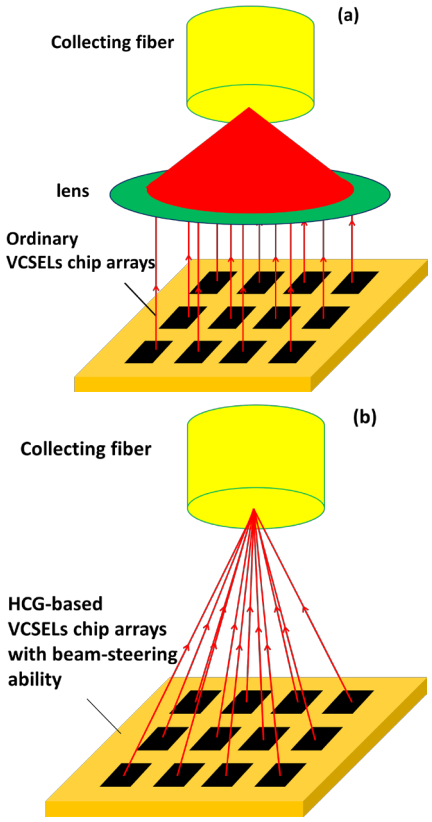

Fig. 1. Light coupling using (a) an ordinary lens and (b) beam-steering HCG.

Designing a HCG with beam-steering ability is straight forward. Given the needed steering angle, such as 30°, an ideal phase distribution can be calculated according to Eq. (2). The next step is to find out the proper grating bars geometric parameters which can introduce a phase profile as Eq. (2). First, transmittivity and phase shift of transmitted light as a function of grating period p and duty cycle η (the ratio of the grating bar width and grating period p) of periodic grating for a certain grating thickness was investigated using the rigorous coupled wave analysis (RCWA)[17] simulation method. Part of these data will be used to design the non-periodic HCG which can achieve a linearly varying phase profile. When varying the grating structure locally, by changing the grating period p and duty cycle η, the phase and transmittivity will change accordingly[15]. So by carefully selecting grating period p and η, we can get a HCG where the phases of the grating-bar centers adapt to Eq. (2). Lu *et al.*[18] pointed out that the transmitted properties of HCG with a discrete phase distribution are good approximation to the ideal case when grating period p is smaller than the wavelength of incident light.

As an example, we will design a HCG with a steering angle of 30°. Here, the HCG consists of high-index silicon (the refractive index is 3.48 at an incident wavelength of 1550 nm), which are completely surrounded

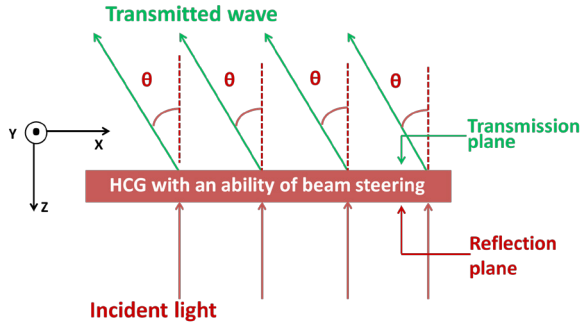

Fig. 2. Schematic diagram of beam steering.

by low-index air (the refractive index is 1 at an incident wavelength of 1550 nm; Fig. 3). The thickness of the HCG is 1.2 μm. Fattal *et al.*[19] provided a detailed method to design a non-periodic HCG.

1. Calculate the transmittivity and phase as a function of (p, η) of periodic HCG using RCWA for transverse magnetic (TM) incident light (the E-field vector is perpendicular to the grating bars) at a wavelength of 1550 nm. The calculation results are shown in Fig. 4. The colorbar in Fig. 4(a) represents the transmittivity which varies from 0 to 1. Moreover, the colorbar in Fig. 4(b) represents the corresponding phase shift which varies from 0 to 2π. Then select part of grating parameters (p, η) with a high transmittivity (such as $|t|^2 > 95\%$) and a gradually changed phase range from 0 to 2π radian. Obtained data are used to selecting grating parameters (p, η) corresponding to the goal phase distribution.

2. Select proper grating parameters (p_n, η_n) from the obtained data in Step 1 for the different coordinates of grating bars center, indicated as x_0, x_1, x_2, ... x_n, ..., one by one to find a discrete phase representation $\Phi(x_n)$ of Eq. (2).

Figure 5 shows the schematic distribution of the designed non-periodic HCG. The relationship between parameters defined in Fig. 5 is described as

$$\begin{cases} x_{n+1} = x_n + \dfrac{1}{2}(p_n + p_{n+1}) \quad , n = 0,1,2,..., \\ \Phi(x_{n+1}) = \Phi\left(x_n + \dfrac{1}{2}(p_n + p_{n+1})\right) \\ \qquad\qquad = k_0 x_{n+1} \sin\theta + c \ , n = 0,1,2,.... \end{cases} \tag{6}$$

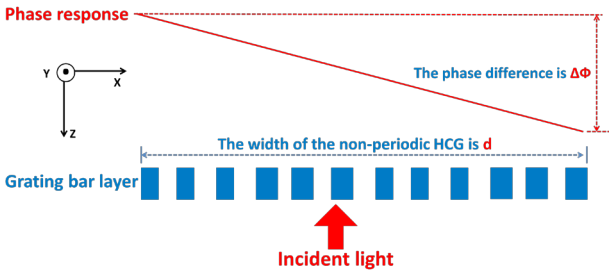

Fig. 3. Schematic of the investigated HCG with a linearly modulated transmission phase response.

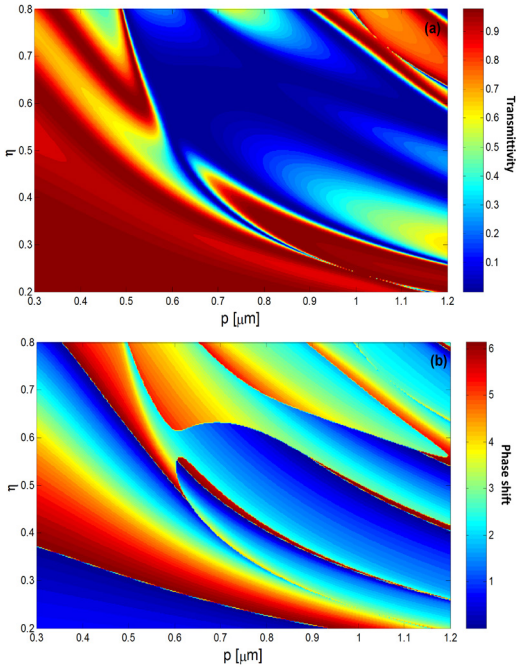

Fig. 4. Maps of (a) transmittivity and (b) phase shift of periodic HCG at the transmission plane.

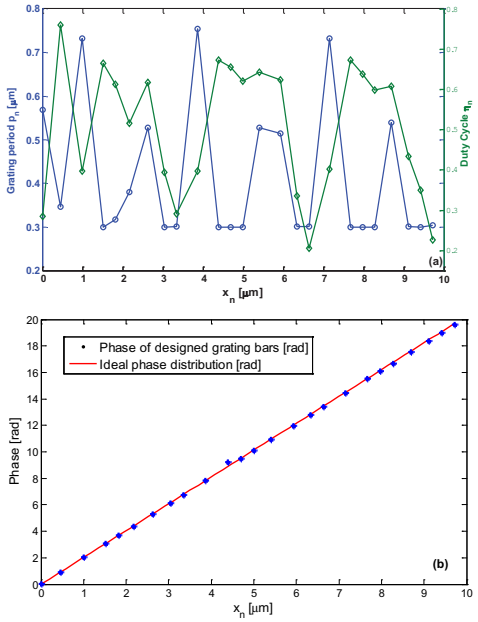

Fig. 6. Maps of (a) (p_n, η_n) and (b) phase shift of the designed non-periodic HCG.

According to the design process, we design a 9.98 μm width HCG with a 30° beam steering. Figure 6 shows the detailed HCG parameters (p_n, η_n) and the corresponding discrete phase distribution. The x-axis represents coordinates of grating bars center. In Fig. 6(a), the blue cycles and green diamonds indicate the discrete grating parameters (p_n, η_n). In Fig. 6(b), the blue spots represent the designed discrete phase shift values which correspond to (p_n, η_n) and the red line is the ideal phase distribution we want to achieve. The grating period p varies from 0.3 to 0.75 μm, and the duty cycle η from 0.2 to 0.8.

The steering properties of the designed HCG are numerically studied using the FEM. The incident light is a TM polarized wave with a Gaussian profile and the wavelength is 1550 nm. In Fig. 7, the simulation domain is depicted. In order to avoiding the reflection interference, the perfectly matched layer (PML) and the scattering boundary condition are used.

The simulation results are indicated in Fig. 8. After the TM polarized light illuminates the designed HCG from the bottom, a number of grating modes in the HCG are excited. Because of the high-refractive-index contrast and sub-wavelength dimensions, only the first two grating modes have real propagation constant in the z direction and have the form of propagating waves. The other higher order grating modes have imaginary propagation constant and have the form of evanescent waves[6]. The thickness and the duty cycle we select make the first two modes interfere constructively at the transmission plane, so high transmission can be achieved. Because of the linear phase modulation, the transmitted light turns to almost the same direction (Fig. 8(a)). Calculation shows that the transmittivity is up to 0.91. Figure 8(b) presents the E-field intensity distribution of the transmission wave at the distances of 14, 16, 18, and 20 μm from the transmission plane. From Fig. 8(b), we find that the peak of E-field intensity profile moves toward the negative x-axis direction. The calculated numerical values of the peaks are shown in Table 1.

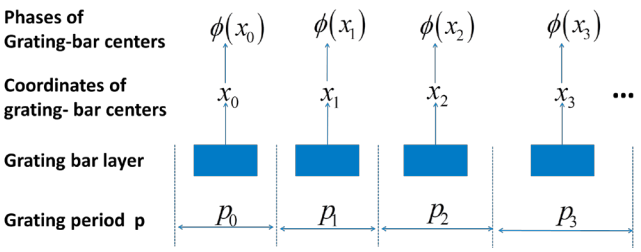

Fig. 5. Schematic of the non-periodic HCG.

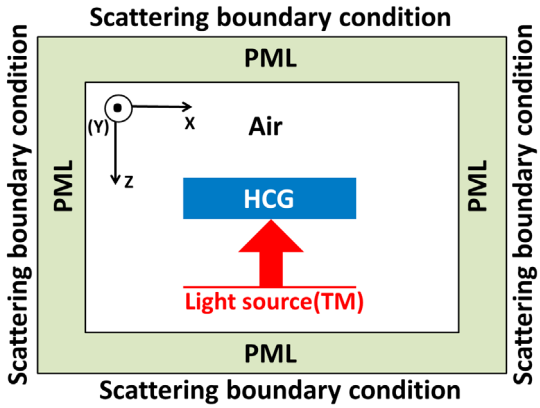

Fig. 7. Sketch of the simulation domain.

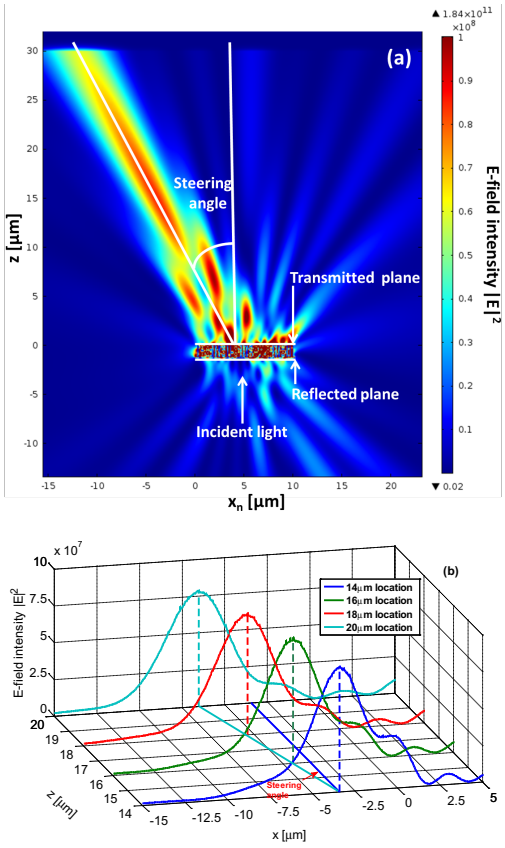

Fig. 8. (a) Distribution of E-field intensity and (b) E-field intensity profile at different distances from transmission plane.

Once the distance from the transmission plane changes from 14 to 20 μm, the electric field intensity profile peak moves $6.53-3.42=3.11$ μm toward lower x coordinates. So the obtained steering angle through the FEM simulation is $\theta=\arctan(3.11/(20-14))=27.42°$, which is close to the theoretical value ~30°. The factor which may contribute to the error is that the phases in the center of the non-periodic grating bars are discrete rather than continuous as indicated by Eq. (2).

In conclusion, we give a rigorous theoretical derivation to the beam-steering principle. Based on this, we present a detailed process of designing high-transmittivity non-periodic HCG with a 30° deflection angle. FEM simulation shows that the transmittivity is up to 0.91 and the deflection angle of the transmitted beam is 27.42°, which is close to the theoretical deflection angle. In the same way, a HCG with arbitrary-angle beam-steering ability can be obtained. Along the same line, a HCG with large-angle beam-steering ability and high reflectivity can be achieved. These kinds of HCGs are easy to fabricate with standard photolithography, and thus can have a significant impact on integrated optics by replacing expensive lens system.

This work was supported by the National Natural Science Foundation of China (Nos. 61274044 and 61077049), the National Basic Research Program of China (No. 2010CB327600), the Specialized Research Fund for the Doctoral Program of Higher Education of China (No. 20130005130001), the Natural Science Foundation of Beijing, China (No. 4132069), the 111 Project (No. B07005), the Program for New Century Excellent Talents in University of Ministry of Education of China (No. NCET-13-0686), and the International Science Cooperation Program (No. 2011DFR11010).

Table 1. Peak Information of the Transmitted Light

Distance from the Transmission Plane (μm)	Peak Intensity ($\lvert E\rvert^2$)	X Coordinate of the Peak (μm)
14	8.5539×10^7	–3.4210
16	8.5124×10^7	–4.4201
18	8.2748×10^7	–5.3724
20	7.8772×10^7	–6.5337

References

1. L. Guo, C. Min, S. Wei, and X. Yuan, Chin. Opt. Lett. **11**, 052601 (2013).
2. V. Karagodsky, F. G. Sedgwick, and C. J. Chang-Hasnain, Opt. Express **18,** 16973 (2010).
3. L. Ge, X. Wang, H. Chen, K. Qiu, and S. Fu, Chin. Opt. Lett. **10**, 090502 (2012).
4. V. Karagodsky and C. J. Chang-Hasnain, Opt. Express **20,** 10888 (2012).
5. R. Zhang, Y. Wang, Y. Zhang, Z. Feng, F. Qi, L. Liu, and W. Zheng, Chin. Opt. Lett. **12**, 020502 (2014).
6. C. J. Chang-Hasnain and W. J. Yang, Adv. Opt. Photon. **4**, 379 (2012).
7. K. Rastani, A. Marrakchi, S. F. Habiby, W. M. Hubbard, H. Gilchrist, and R. E. Nahory, Appl. Opt. **30,** 1347 (1991).
8. T. Fujita, H. Nishihara, and J. Koyama, Opt. Lett. **7**, 578 (1982).
9. R. Magnusson and M. Shokooh-Saremi, Opt. Express **16,** 3456 (2012).
10. T. Shiono, M. Kitagawa, K. Setsune, and T. Mitsuyu, Appl. Opt. **28**, 3434 (1989).
11. C. Chase, Y. Rao, W. Hofmann, and C. J. Chang-Hasnain, Opt. Express **18**, 15461(2010).
12. S. Boutami, B. Benbakir, J. L. Leclercq, and P. Viktorovitch, Appl. Phys. Lett. **91**, 071105 (2007).
13. A. J. Liu, W. Hofmann, and D. Bimberg, Opt. Express **22**, 11804 (2014).
14. Y. Zhou, M. C. Y. Huang, and C. J. Chang-Hasnain, IEEE Photon. Technol. Lett. **20**, 434 (2008).
15. L. Carletti, R. Malureanu, J. Mrøk, and I. S. Chung, Opt. Express **19,** 23567 (2011).
16. O. C. Zienkiewicz and R. L. Taylor, *The Finite Element Method: Basic Formulation and Linear Problems* (McGraw-Hill, 2005).
17. M. G. Moharam and T. K. Gaylord, J, Opt. Soc. Am. A **71**, 811 (1981).
18. F. Lu, F. G. Sedgwick, V. Karagodsky, C. Chase, and C. J. Chang-Hasnain, Opt. Express **18**, 12606 (2010).
19. D. Fattal, J. J. Li, and Z. Peng, Nat. Photon. **4,** 466 (2010).